Mathematical Biosciences and Engineering

http://www.aimspress.com/journal/MBE

MBE, 18(4): 4648–4678.
DOI: 10.3934/mbe.2021236
Received: 04 April 2021
Accepted: 20 May 2021
Published: 27 May 2021

Research article

A hybrid equilibrium optimizer algorithm for multi-level image segmentation

Hong Qi [1], **Guanglei Zhang** [1,*], **Heming Jia** [2] **and Zhikai Xing** [3]

[1] School of Information and Computer Engineering, Northeast Forestry University, China
[2] School of Information Engineering, Sanming Universiy, China
[3] School of Electrical Engineering and Automation, Wuhan University, China

* **Correspondence:** zhangguanglei@nefu.edu.cn.

Abstract: Threshlod image segmentation is a classic method of color image segmentation. In this paper, we propose a hybrid equilibrium optimizer algorithm for multi-level image segmentation. When multi-level threshold method calculates the neighborhood mean and median of color image, it takes huge challenge to find the optimal threshold. We use the proposed method to optimize the multi-level threshold method and get the optimal threshold from the color image. In order to test the performance of the proposed method, we select the CEC2015 dataset as the benchmark function. The result shows that the proposed method improves the optimization ability of the original algorithm. And then, the classic images and wood fiber images are taken as experimental objects to analyze the segmentation result. The experimental results show that the proposed method has a good performance in Uniformity measure, Peak Signal-to-Noise Ratio and Feature Similarity Index and CPU time.

Keywords: wood fiber image segmentation; 3DOtsu; equilibrium optimizer algorithm; grasshopper optimization algorithm; hybrid optimization algorithm

1. Introduction

Image segmentation is the basic work of image processing research. There are primarily four types of segmentation methods: thresholding [1–3], boundary-based [4,5], region-based [6–8], and hybrid techniques [9–12]. Several algorithmic techniques such as Artificial Neural Network [13], Convolutional neural Network [14], and K-nearest Neighbors [15] can also be applied in image segmentation.

Among all the methods of image segmentation, Otsu [16] method is the most popular one. Computational complexity of Otsu methods increases exponentially with the increasing number of thresholds due to exhaustive search. It is a difficult task to study how to improve the segmentation accuracy of Otsu with multi-thresholds method. The expansion of the actual Otsu's thresholding to multilevel thresholding is known as multi-Otsu thresholding [17]. Nevertheless, these methods are unable to obtain effective results for noisy images. To solve this problem, J. Zhuang [18] proposed a 2-D Otsu method that selects the optimal threshold on a 2-D histogram. Jing [19] proposed the maximum between-cluster variance by using a 3-D histogram approach and was named the 3-D Otsu method. In this method, the 3D histogram takes the median value of neighborhood pixels as the third feature of the existing features of the 2D OTSU method, that is, gray information and neighborhood mean value. L. Wang [20] derived a group of recurrence formula for 3-D Otsu's method and eliminated redundancy in the formula by introducing a look-up table. The method reduced the computation of the 3DOtsu. Therefore, in order to optimize the search process, a faster and automatic optimal threshold selection method is needed.

The traditional exhaustive methods take the large amount of computation. In this case, meta-heuristic methods have attracted much attention in recent years. L. Bian proposed a new multi-threshold MRI image segmentation algorithm based on mixed entropy using Curvelet transformation and Multi-Objective Particle Swarm Optimization [21]. This method could deal with the difficulties caused by noise disturbance, intensity inhomogeneity and edge blurring in Magnetic Resonance Imaging image segmentation. N. Muangkote proposed the nature-inspired meta-heuristic named multilevel thresholding moth-flame optimization algorithm (MTMFO) for multilevel thresholding [22]. This algorithm effectively solved the problem of satellite image segmentation. B. Surina proposed a multi-level thresholding model based on gray-level & local-average histogram (GLLA) and Tsallis–Havrda–Charvát entropy for RGB color image [23]. This method had the effectiveness and reasonability. A. Wunnava proposed an adaptive Harris Hawks optimization (AHHO) technique to solve the multi-level image segmentation [24]. The experimental results were beneficial to the segmentation field of image processing. The optimization algorithm is adopted to solve the threshold selection of the multi-threshold image segmentation method, which effectively improves the segmentation precision of the image segmentation method [25,26].

The optimization algorithm can solve practical engineering problems in recent years [27]. Different optimization algorithms adapt to different engineering problems and have different optimization capabilities [28,29]. These nature-inspired optimization algorithms were mainly classified into two classes recently which are evolutionary algorithm (EA) and biology-inspired or bio-inspired algorithms. EA imitated the Darwinian theory of evolution [30]. There were many good algorithms in this class. In 1975, GA was invented by John Holland [31], it used the binary representation of individuals. In 1997, Differential evolution was proposed Rainer stone, the essence was a multi - objective optimization algorithm [32]. The most popular class was the biology-inspired or bio-inspired algorithms right now. One of the most famous algorithms was the Particle Swarm Optimizer (PSO) which was developed based on the swarming behavior of fish and birds [33]. In 2015, the ant lion optimizer was proposed by Mirjalili [34]. In 2016, Askarzadeh proposed the crow search algorithm [35]. In 2017, the killer whale algorithm was proposed by Biyanto [36]. These algorithms were inspired from the predation behavior animal, so as to obtain better searching ability. There also some algorithms inspired from the physics and chemistry, these algorithms usually had simple mathematical models, but had good optimization effect. In 2001, the harmony search algorithm was proposed by Geem [37]. In 2015, Zheng Yu-Jun proposed water wave optimization algorithm [38]. In 2019, A. Faramarzi proposed a novel optimization algorithm, called Equilibrium optimizer (EO), which controlled volume mass balance models used to estimate both dynamic and equilibrium states [39]. No-Free-Lunch [40] proved that no algorithm can solve all optimization problems.

There is no perfect optimization algorithm and the optimization algorithm should be improved to better solve engineering problems. Many scholars study the hybrid optimization algorithm [41]. Pankaj U. proposed a new multistage hybrid optimization algorithm to optimize multilevel threshold [42]. The method had a good performance in test images. Amandeep proposed a fast SAR image segmentation method based on Particle Swarm Optimization-Gravitational Search Algorithm [43]. The method had good segmentation accuracy. D. Kole proposed a new approach to automatic unsupervised efficient image segmentation algorithm using hybrid technique based on Particle Swarm Optimization and Genetic Algorithm [44]. Gao H. presented a learning strategy-based particle swarm optimization algorithm with an exchange method [45]. The experiment shows that the method had a good result using the Berkeley images. So, the hybrid optimization algorithm could use the advantage of the different algorithms to enhance the search ability of the original algorithm.

This paper focuses on the segmentation of wood fiber images. The wood fiber images have the small target, it takes huge challenge for the segmentation method. We use 3DOtsu as a fitness function to segment wood fiber images. The threshold image method can overcome the difficulty of wood fiber image difference channel. The Equilibrium optimizer algorithm can find the threshold of the wood fiber images, however the segmentation accuracy is low and the CPU time is large. In order to improve the optimal ability of EOA, we use the GOA improve the EOA. The HEOA obtains the strong ability find the optimal threshold from the wood fiber images.

In this paper, the HEOA is proposed. The main contribution of this study is that the GOA improves the original EOA for multilevel threshold. Experiments are performed on CEC2015 data, classic images and wood fiber images. The proposed algorithm is compared with the original EOA and other six algorithms include CSA, FPA, PSO, HSOA and HWOA. The GOA algorithms can balance the exploration and exploitation of the EOA. The results show the superiority of the proposed algorithm in terms of the objective function value, image quality measures on both normal and high-level thresholding.

2. Materials and methods

2.1. Otsu's Function

Otsu algorithm is a classical image segmentation method, and its segmentation results are excellent. This method can be extended to multi-threshold Otsu to obtain the maximum variance between two classes, so as to obtain the optimal threshold of the image [46].

Assuming that there are *K* thresholds, which divide the image into *K+1* classes. The extended between-class variance is calculated by

$$f(t) = \sum_{i=0}^{K} \sigma_i \tag{1}$$

The sigma terms are determined by Eq. (6) and the mean levels are calculated by Eq. (7):

$$\sigma_0 = \varpi_0(\mu_0 - \mu_T)^2,\ \sigma_1 = \varpi_1(\mu_1 - \mu_T)^2,\ \cdots,$$
$$\sigma_{K-1} = \varpi_{K-1}(\mu_{K-1} - \mu_T)^2 \tag{2}$$

$$\mu_0 = \sum_{i=1}^{t} ip_i /\varpi_0, \;\; \mu_1 = \sum_{i=t_1+1}^{t_2} ip_i /\varpi_1, \;\; \cdots,$$

$$\mu_{K-1} = \sum_{i=t_{M-1}+1}^{L} ip_i /\varpi_{K-1} \tag{3}$$

The optimum thresholds are found by maximizing the between-class variance by Eq. (8):

$$t^* = argmax(\sum_{i=0}^{K-1} \sigma_i) \tag{4}$$

2.2. 3DOtsu's Function

3D-Otsu, the histogram is constructed by taking gray values of pixels along with their spatial information including the neighborhood mean and median [47]. The Otsu only segment the single channel of the image, however the color images have three channels. There are more information in the three channels, so the 3DOtus can use the information of three channels and get the best threshold form the color images. An image I with K gray levels and N number of pixels is considered, where the intensity value of pixel at the location (x, y) denoted by$f(x, y)$. The mean and median value of $l \times l$ neighborhood of pixel is denoted by$g(x, y)$ and$h(x, y)$, which is defined by Eq. (9) and Eq. (10).

$$g(x,y) = \frac{1}{l^2} \sum_{i=-\frac{l-1}{2}}^{\frac{l-1}{2}} \sum_{j=-\frac{l-1}{2}}^{\frac{l-1}{2}} f(x+i, y+j) \tag{5}$$

$$h(x,y) = med\left\{f(x+i, y+j); i,j = -\frac{l-1}{2}, \ldots, \frac{l-1}{2}\right\} \tag{6}$$

Where, the value of *l* is taken as 3 in this paper. For every pixel in the image *I*, mean and median values are calculated in the $l \times l$ neighborhood.

Let (t_f, t_g, t_h) as the optimal threshold of the three histograms, and use the Eq. (8) to calculate the optimal threshold from the three histograms. The optimal threshold is expressed as:

$$t_f^* = argmax\{\sum_{i=0}^{K-1} \sigma_i(t_f)\} \tag{7}$$

$$t_g^* = argmax\{\sum_{i=0}^{K-1} \sigma_i(t_g)\} \tag{8}$$

$$t_h^* = argmax\{\sum_{i=0}^{K-1} \sigma_i(t_h)\} \tag{9}$$

The final optimum thresholds are average of the result of t_f^*, $t_g^*$and $t_\hbar^*$, and can be defined by Eq.10:

$$t^* = (t_f^* + t_g^* + t_h^*)/3 \tag{10}$$

The 3DOtsu image segmentation method uses the information of three channels of color images, the optimal threshold can segment the image exactly.

2.3. Equilibrium optimizer algorithm

The EO method is inspired by the simple well-mixed dynamic mass balance on the control body, in which the mass balance equation is used to describe the coordination of non-active components in the control body as a function of its various source and aggregation mechanisms. Similar to most meta-heuristic algorithms, EO uses the initial population to start the optimization process. The equilibrium candidates' collaboration can be seen from Figure1. The initial concentrations are constructed based on the number of particles and dimensions with uniform random initialization in the search space as follows:

$$C_i^{initial} = Cminmax_{min} \tag{11}$$

Where, $C_i^{initial}$is the initial concentration vector of the ith particle, $C_{max}$and C_{min}denote the minimum and maximum values for the dimensions, rand is a random vector in interval of [0, 1].

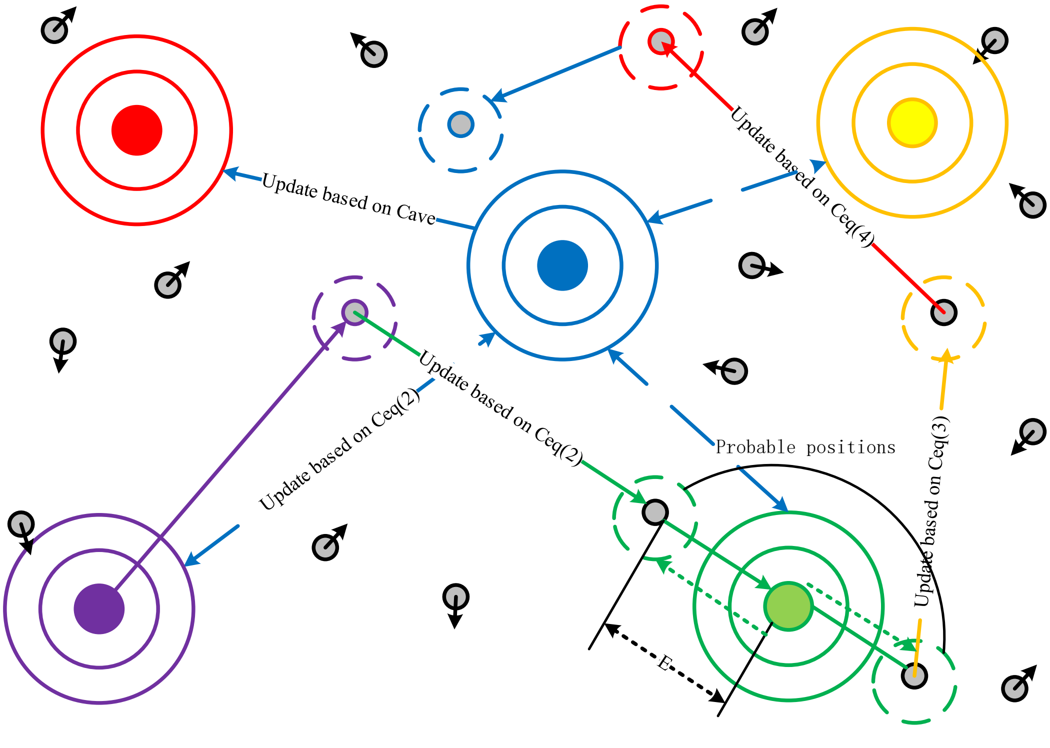

Figure 1. Equilibrium candidates' collaboration.

The equilibrium state is the final convergence state of the algorithm, which is desired to be the global optimum. At the beginning of the optimization process, there is no knowledge about the equilibrium state and only equilibrium candidates are determined to provide a search pattern for the particles. According to the different experiments under different types of case problems, these candidate particles are the four optimal particles determined in the whole optimization process plus another particle. These particles are nominated as equilibrium candidates and are used to construct a vector called the equilibrium pool:

$$\vec{C}_{eq,pool} = \{\vec{C}_{eq(1)}, \vec{C}_{eq(2)}, \vec{C}_{eq(3)}, \vec{C}_{eq(4)}, \vec{C}_{eq(ave)}\} \tag{12}$$

Where, $\vec{C}_{eq(1)}$ is the first particle updates all of its concentrations, $\vec{C}_{eq(ave)}$is the average of the particle.

The main concentration updating rule is the exponential term (F). In order to guarantee convergence by slowing down the search speed along with improving the exploration and exploitation ability of the algorithm, the version can be seen as:

$$\vec{F} = a_1 \times sign(r - 0.5) \times (e^{-\lambda \times t} - 1) \tag{13}$$

Where:

$$t = (1 - \frac{Iter}{Max\_iter})^{(a_2 \frac{Iter}{Max\_iter})} \tag{14}$$

Where, *Iter* and *Max_iter* present the current and the maximum number of iterations.

The generation rate is one of the most important terms in the proposed algorithm to provide the exact solution by improving the exploitation phase. The final set of generation rate equation is as follows:

$$\vec{G} = \vec{G_0} e^{-\lambda \times (t - t_0)} = \vec{G_0} - \vec{F} \tag{15}$$

Where:

$$\vec{G_0} = \vec{GCP} (\vec{C_{eq}} - \lambda \vec{C}) \tag{16}$$

$$\vec{GCP} = \begin{cases} 0.5 r_1 & r_2 \geq GP \\ 0 & r_2 < GP \end{cases} \tag{17}$$

Where, $r_1$and$r_2$are random numbers in [0, 1] and GCP vector is constructed by the repetition of the same value resulted from Eq. (16).

Finally, the updating rule of EO will be as follows:

$$\vec{C} = \vec{C_{eq}} + (\vec{C} - \vec{C_{eq}}) \times \vec{F} + \frac{\vec{G}}{\lambda V} (1 - \vec{F}) \tag{18}$$

Where, *F* is defined in Eq. (13), and *V* is considered as unit.

2.4. Mathematical model of GOA

In 2017, Mirjalili Seyedali proposed the grasshopper optimization algorithm [48]. The grasshoppers are a genus of straight fins of insect, they are seen as pests, because they are in crops for food, to cause damage to agriculture. The growth cycle of grasshoppers is shown in Figure 2. The grasshoppers usually exist alone in nature, but they are one of the biggest swarm of all species. The grasshoppers are unique in that they crowd behavior in adults and larvae of between. Millions of larva foraging on the basis of jumping, they feed on almost all plants, and when they reach adulthood, they form a large group in the air, making long migrations, looking for the next food source.

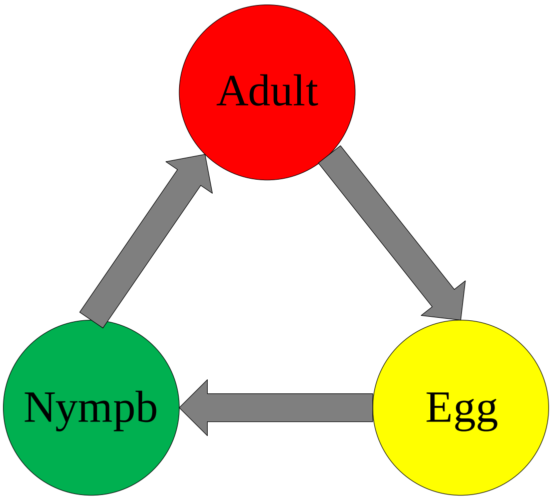

Figure 2. Grasshopper growth cycle.

In larvae stage, the main characteristic of grasshopper is moving slowly, small scale food. When they become adult, collective action has became the main activity characteristics of grasshopper. The natureinspired algorithms logically divide the search process into two tendencies: exploration and exploitation. So mathematical model of the gregarious grasshoppers is represented as follows:

$$X_i = S_i + G_i + A_i \tag{19}$$

where $X_i$defines the position of the i-th grasshopper, $S_i$is the social interaction, $G_i$is the gravity force on the i-th grasshopper, and $A_i$shows the wind advection.

$$\begin{cases} S_i = \sum_{j=1}^{N} s(d_{ij})\vec{d}_{ij} \\ s(r) = fe^{\frac{-r}{l}} - e^{-r} \end{cases} \tag{20}$$

where d_{ij} is the distance between the i-th and the j-th grasshopper, calculated as $d_{ij} = |x_j - x_i|$, s is a function to define the strength of social forces, $\vec{d}_{ij}$ is an unit vector from the i-th grasshopper to the j-th grasshopper.

$$G_i = -g\vec{e}_g \tag{21}$$

where g is the gravitational constant and $\vec{e}_g$ shows an unity vector towards the center of earth.

$$A_i = u\vec{e}_w \tag{22}$$

Where u is a constant drift and $\vec{e}_w$ is a unity vector in the direction of wind.

Substituting S, G, and A into Eq. (19), then this equation can be expanded as follows:

$$X_i = \sum_{j=1}^{N} s(|x_j - x_i|)\frac{x_j - x_i}{d_{ij}} - g\vec{e}_g + u\vec{e}_w \tag{23}$$

However, this mathematical model cannot be used directly to solve optimization problems, mainly because the grasshoppers quickly reach the comfort zone and the swarm does not converge to a specified point. A modified version of this equation is proposed as follows to solve optimization problems:

$$X_i^d = c_1\left(\sum_{j=1}^{N} c_2 \frac{ub_d - lb_d}{2} s(|x_j - x_i|) \frac{x_j - x_i}{d_{ij}}\right) + \vec{T}_d \tag{24}$$

Among them, $ub_d$and lb_d are a type of upper and lower limitation, $\vec{T}_d$is the optimal value after each iteration, $c_1 = c_2 = c\,max - l\frac{c\,max - cmin}{L}$, $c_1$balances the global search and local search for the target area, c_2 balances the relationship among the attraction between two grasshopper, *cmax* and *cmin* can set the maximum and minimum search ability, l represents the current iteration number, L is the largest number of iterations.

2.5. The proposed method

In this subsection, we describe the hybrid equilibrium optimizer algorithm in detail. The EOA fall into the local optimal easily. The algorithm cannot balance the exploitation and exploration. In order to solve this problem, we use the advantage of the GOA to improve the optimization ability of the GOA. We use the Eq. (19) to enhance the individual ability of the EOA. The X_i have the strong ability to avoid the EOA drop into the local optimal. The formula can be seen below:

$$\vec{C} = \vec{C}_{eq} + (\vec{C} - \vec{C}_{eq}) \times \vec{F} + \frac{\vec{G}}{\lambda V}(1 - \vec{F}) \times X_i \tag{25}$$

A comprehensive algorithm step of HEOA based multilevel color image segmentation is given in Algorithm 1.

Algorithm 1 Pseudo-code of HEOA algorithm

```
Input: The color image
Output: Segmentation color image
Read the input and compute the histogram of three channels of color image
Initialize the parameters $r_1$and$r_2$
Initialize the random population $C_i$
while L < Max_iter do
        Calculate the fitness values of EOA
        for (each hawk $C_i$) do
            Calculate $C_{eq}$,$X_i$
            Update the C using Eq. (25)
            Calculate the fitness function using Eq.(10)
        end for
        Update$C_{best}$if there is a better solution
        L=L+1
end while
Get the best solution as the multilevel threshold K
According the K segment the three channels of the images
Get the segmentation images
```

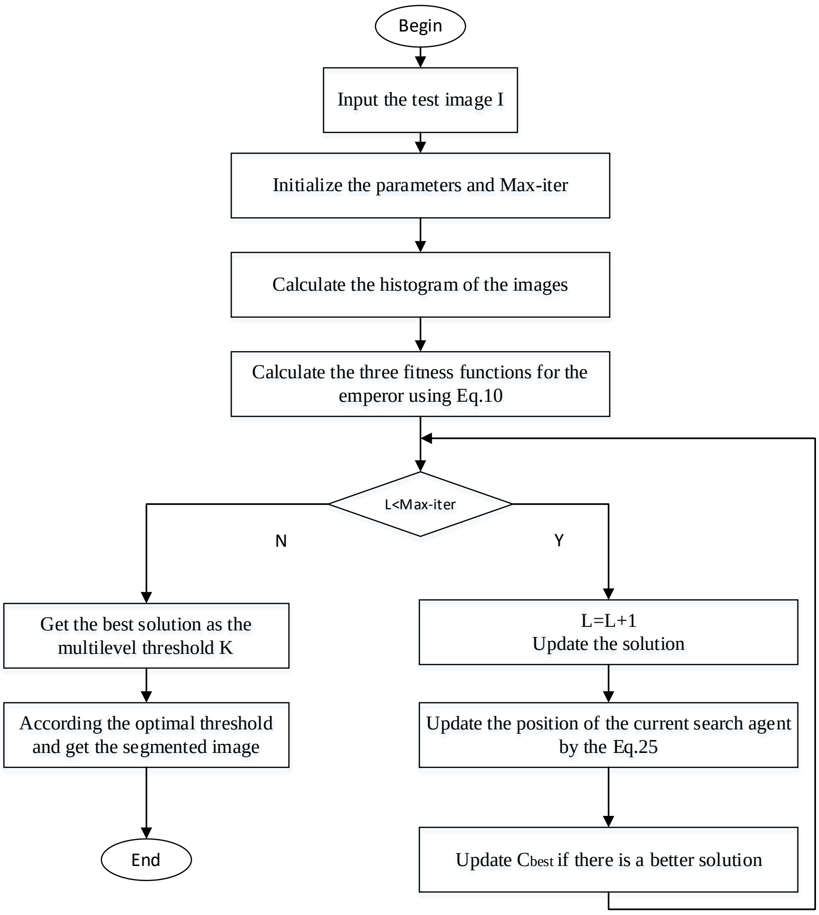
Begin
Input the test image I
Initialize the parameters and Max-iter
Calculate the histogram of the images
Calculate the three fitness functions for the emperor using Eq.10
L<Max-iter
N
Y
Get the best solution as the multilevel threshold K
According the optimal threshold and get the segmented image
End
L=L+1
Update the solution
Update the position of the current search agent by the Eq.25
Update Cbest if there is a better solution

Figure 3. The flowchart of proposed method.

In order to use the information of the three channels of color images, we use the fitness functions Eq. (10) to calculate the histogram of the three channels. And then, we use the HEOA to optimize the fitness function. Finally, we can get the best threshold and segment the color images. The flowchart of the BMPA can be seen from the Figure 3.

The computational complexity of the proposed method depends on the number of each combination (L), the number of generations (g), the number of population (n) and the parameters dimensions (d). So, computational complexity on L combination is $O(L)$. The computational complexity of population location update is O(n*d). The calculation of fitness function values of all seagull populations is$O(n^*L)$. Therefore, the final computational complexity of the proposed method is:

$$O(MBE) \approx O(g^*(n^*d + n^*L)) \tag{26}$$

3. Benchmark function experiments and results

To verify the optimization performance of HEOA, its performance is compared with five other optimization methods including CSA, FPA, PSO, BA and basic EOA. The optimization algorithm compared in this section tests CEC2015 benchmark test functions. The detailed description of CEC 2015 benchmark test functions [49] is presented in Table 2. For fair comparison, the other parameters of all algorithms are set according to their original papers. The results obtained by the algorithms on benchmark functions are presented in Table 3. All parameters of the comparison optimization algorithm are shown in table 1. Figure 4 show the result of the CEC2015. The population size is 30 and the number of iterations is 100. The proposed DLNN are testing in Matlab 2018b.

Table 1. Parameters and references of the comparison algorithms.

Algorithm	Parameters	Value
EOA	c_1	2
	c_2	2
CSA [50]	AP	0.5
FPA [51]	P	0.5
PSO [52]	Swam size	200
	Cognitive, social acceleration	2,2
	Inertial weight	0.95–0.4
BA [53]	β	(0,1)
HEOA	Levy	1.5

As can be seen from table 3, the results of HEOA algorithm in processing all standard functions are better than those of other comparison algorithms, indicating that the HEOA algorithm can not only solve single-dimensional mathematical functions but also deal with multi-dimensional mathematical functions effectively. It shows that the optimization ability of HEOA algorithm is superior to other comparison algorithms. It can be seen from the Figure 4, the EOA and BA obtains the worst result and the HEOA gets the best result. Above the analysis, HEOA obtains the strong optimal ability, and in the next section we use the HEOA optimize the 3DOtsu.

Table 2. CEC 2015 benchmark test functions.

No.	Functions	Related basic functions	Dim	fmin
CEC-1	Rotated Bent Cigar Function	Bent Cigar Function	30	100
CEC-2	Rotated Discus Function	Discus Function	30	200
CEC-3	Shifted and Rotated Weierstrass Function	Weierstrass Function	30	300
CEC-4	Shifted and Rotated Schwefel's Function	Schwefel's Function	30	400
CEC-5	Shifted and Rotated Katsuura Function	Katsuura Function	30	500
CEC-6	Shifted and Rotated HappyCat Function	HappyCat Function	30	600
CEC-7	Shifted and Rotated HGBat Function	HGBat Function	30	700
CEC-8	Shifted and Rotated Expanded Griewank's plus Rosenbrock's Function	Griewank's Function Rosenbrock's Function	30	800
CEC-9	Shifted and Rotated Expanded Scaer's F6 Function	Expanded Scaer's F6 Function	30	900
CEC-10	Hybrid Function 1 (N = 3)	Schwefel's Function Rastrigin's Function High Conditioned Elliptic Function	30	1000
CEC-11	Hybrid Function 2 (N = 4)	Griewank's Function Weierstrass Function Rosenbrock's Function Scaer's F6 Function	30	1100

CEC-12	Hybrid Function 3 (N = 5)	Katsuura Function HappyCat Function Expanded Griewank's plus Rosenbrock's Function Schwefel's Function Ackley's Function	30	1200
CEC-13	Composition Function 1 (N = 5)	Rosenbrock's Function High Conditioned Elliptic Function Bent Cigar Function Discus Function High Conditioned Elliptic Function	30	1300
CEC-14	Composition Function 2 (N = 3)	Schwefel's Function Rastrigin's Function High Conditioned Elliptic Function	30	1400
CEC-15	Composition Function 3 (N = 5)	HGBat Function Rastrigin's Function Schwefel's Function Weierstrass Function High Conditioned Elliptic Function	30	1500

Table 3. The result of the compared algorithms.

Func.	HEOA		CSA		PSO		FPA		BA		EOA	
	Mean	Std.	Mean	Std.	Mean	Std.	Mean	Std.	Mean	Std.	Mean	Std.
CEC-1	1.05E+05	1.54E+07	4.21E+05	1.47E+08	2.17E+09	3.53E+07	1.76E+08	7.02E+07	4.76E+08	2.86E+08	1.07E+05	3.69E+07
CEC-2	6.70E+06	1.70E+09	2.06E+04	5.26E+09	7.01E+10	3.53E+09	3.04E+10	4.70E+09	3.36E+10	6.82E+09	6.70E+07	4.05E+09
CEC-3	3.20E+02	7.12E-02	3.20E+02	1.51E-01	3.22E+02	9.57E-02	3.21E+02	1.43E-01	3.21E+02	2.10E-01	3.55E+02	1.47E-01
CEC-4	4.10E+02	1.75E+00	4.05E+02	9.03E+00	5.46E+02	1.29E+01	5.30E+02	1.61E+01	5.21E+02	9.70E+00	4.50E+02	2.39E+01
CEC-5	9.81E+02	1.50E+02	1.22E+03	3.30E+02	4.74E+03	2.40E+02	3.80E+03	3.97E+02	3.65E+03	3.52E+02	9.91E+02	2.97E+02
CEC-6	2.05E+03	4.75E+06	2.14E+03	2.33E+07	3.79E+09	9.03E+06	4.52E+09	1.14E+07	1.28E+08	2.71E+07	2.10E+03	1.37E+07
CEC-7	7.02E+02	1.24E+01	7.03E+02	4.37E+01	1.81E+03	1.40E+01	1.78E+03	2.70E+01	1.78E+03	4.99E+01	8.82E+02	2.49E+01
CEC-8	1.47E+03	1.03E+06	1.41E+04	3.25E+06	2.21E+09	1.05E+06	1.34E+09	1.63E+06	1.34E+09	3.78E+06	1.47E+04	1.08E+06
CEC-9	1.00E+03	7.30E+00	1.00E+03	4.77E+01	1.33E+03	2.45E+01	1.33E+03	3.46E+01	1.62E+03	5.15E+01	1.00E+04	3.38E+01
CEC-10	1.23E+03	4.82E+04	2.05E+03	3.09E+06	2.58E+09	4.14E+05	2.97E+07	8.13E+05	4.41E+08	4.49E+06	1.36E+04	7.89E+05

CEC-11	1.35E+03	4.52E+01	1.40E+03	7.94E+01	2.00E+03	6.39E+01	1.77E+03	1.02E+02	1.77E+03	9.80E+01	1.32E+04	1.24E+02
CEC-12	1.30E+03	1.03E+01	1.30E+03	1.75E+01	1.76E+03	1.22E+01	1.49E+03	1.28E+01	1.51E+03	3.25E+01	1.34E+05	1.58E+01
CEC-13	1.30E+03	8.67E+00	1.34E+03	1.49E+00	5.44E+05	1.86E+01	1.54E+03	3.03E+01	1.56E+03	2.48E+00	1.55E+05	3.24E+01
CEC-14	3.22E+03	2.32E+03	8.88E+03	4.24E+03	2.23E+04	2.92E+03	2.23E+04	4.76E+03	2.23E+04	5.46E+03	3.22E+04	3.59E+03
CEC-15	1.60E+03	3.36E+02	1.60E+03	6.49E+02	1.28E+04	7.10E+02	9.01E+03	1.34E+03	4.09E+03	1.05E+03	1.80E+03	1.27E+03

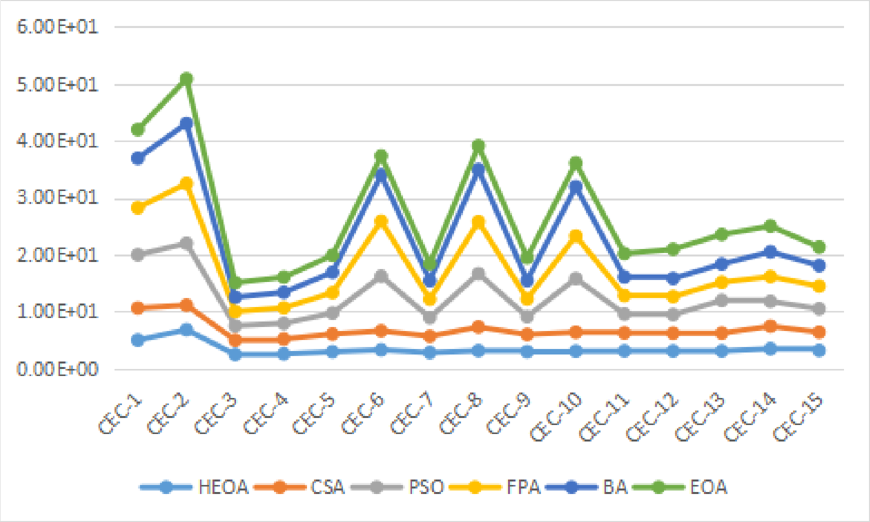

Figure 4. The result of CEC2015.

4. Color image segmentation experiment

In this section, HEOA algorithm is applied to optimize the 3DOtsu. In order to better verify the image segmentation ability of proposed algorithm, it is compared with the optimized 3DOtsu algorithm of CSA, PSO, FPA and BA. The color image has three color channels. In this paper, the images of the three channels are segmented, and then the three resulting images are fused to obtain the final segmentation result graph. Firstly, the segmentation effect and precision of HEOA algorithm are analyzed when the threshold value is increased. Then the segmentation ability, statistical analysis and stability analysis of the proposed HEOA algorithm and other optimization algorithms in 3DOtsu image segmentation are analyzed. All parameters of the comparison optimization algorithm are shown in table 3. The test images and the histogram of three channels of color images are as follows Figure 5. The test images included color natural images and satellite images. It can be seen from the histogram, the histogram of three channels has significant different and it take huge challenge for optimization algorithm to find the optimal threshold. Color image segmentation requires a higher threshold level, so it is more complex to use optimization technology to solve the problem. Therefore, the optimization algorithm has the characteristics of randomness.

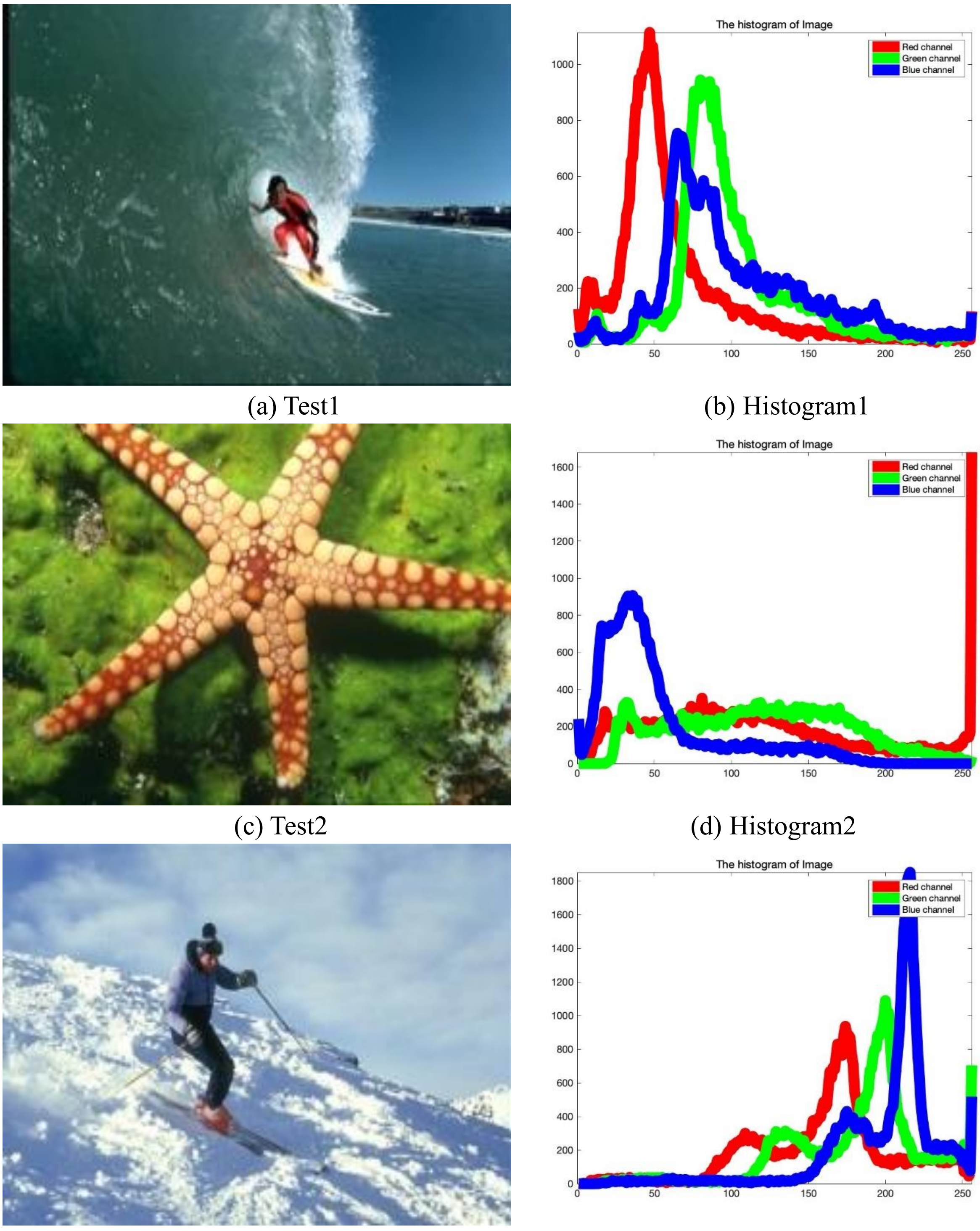

(a) Test1

(b) Histogram1

(c) Test2

(d) Histogram2

(e) Test3

(f) Histogram3

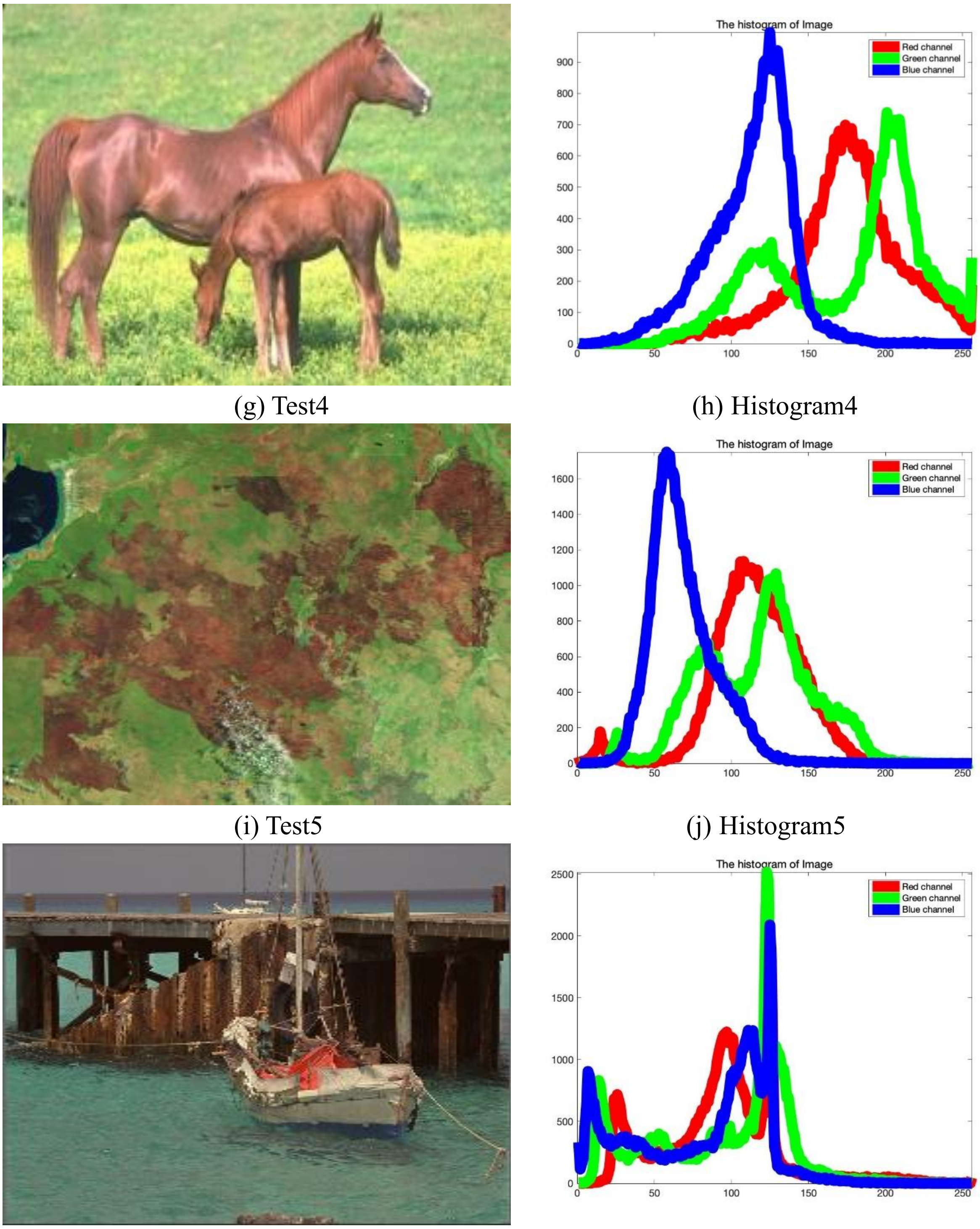

(g) Test4

(h) Histogram4

(i) Test5

(j) Histogram5

(k) Test6

(l) Histogram6

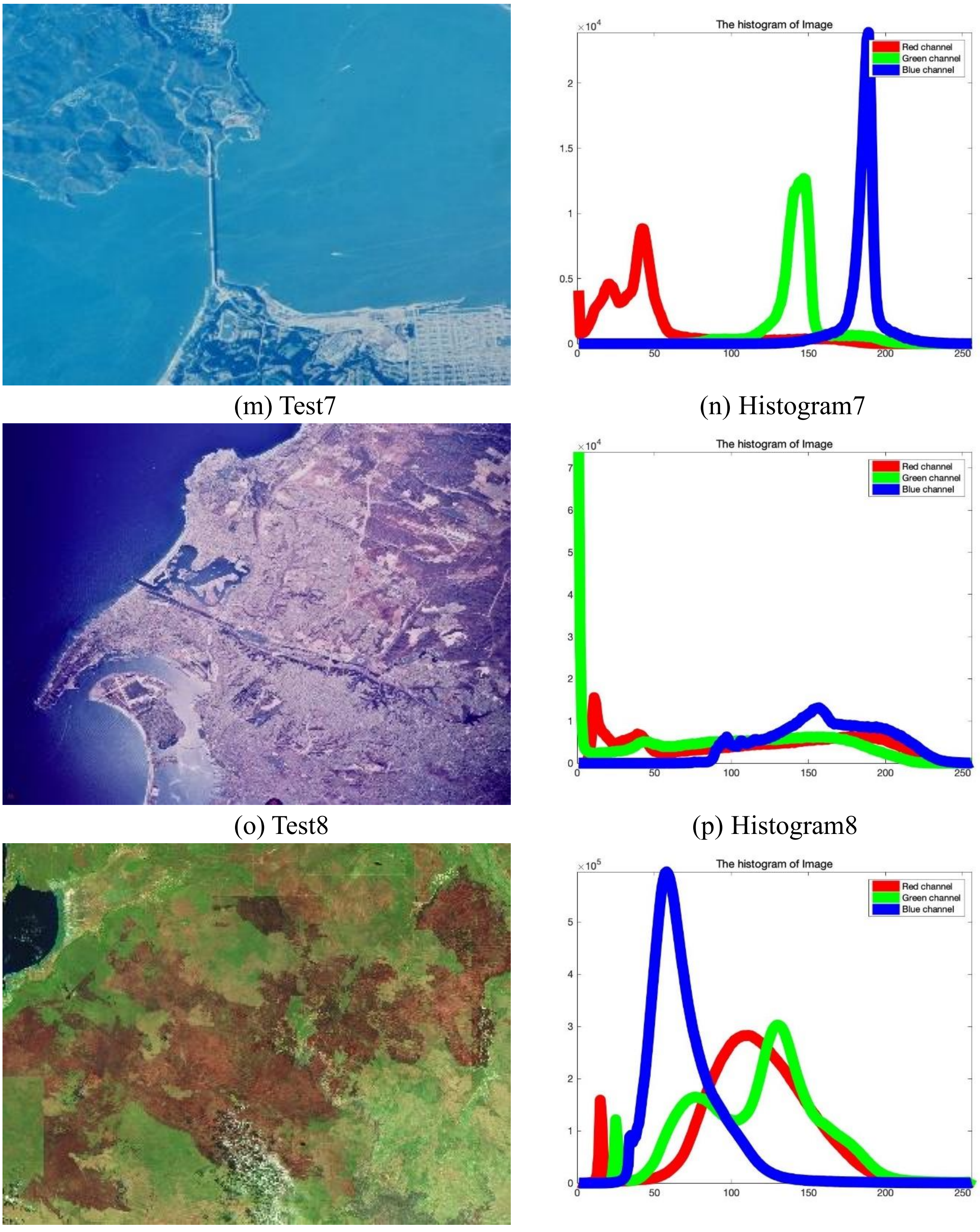

(m) Test7

(n) Histogram7

(o) Test8

(p) Histogram8

(q) Test9

(r) Histogram9

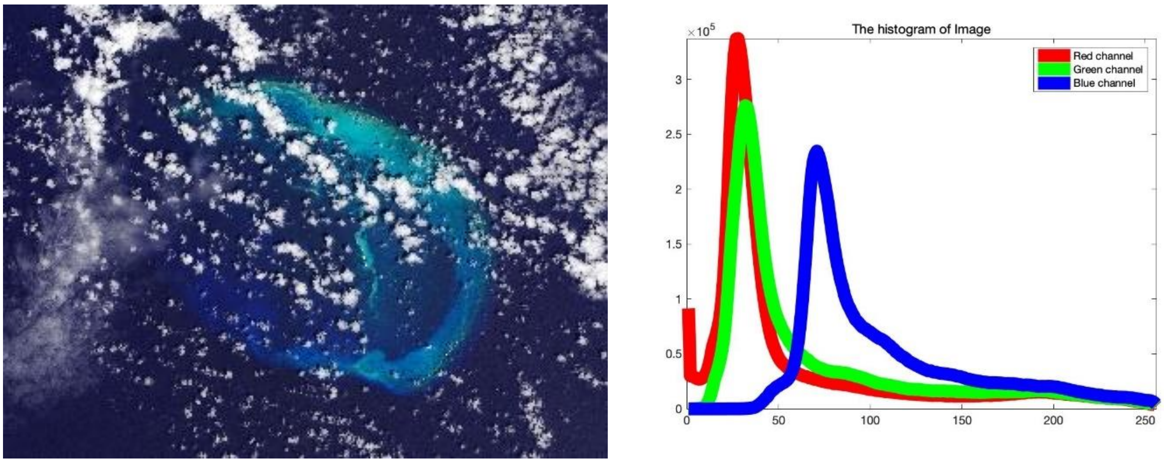

(s) Test10 (r) Histogram10

Figure 5. The color test images and histogram.

In order to better observe the performance of the algorithm, we select K = 4, 8, 12 and 15. The evaluation index can better observe the performance of the algorithm. In order to comprehensively analyze the performance of the algorithm, we calculate the CPU time, Uniformity (U), Peak Signal-to-Noise Ratio (PSNR) and Feature Similarity Index (FSIM). The evaluation index of many object optimization methods can be seen table 4.

Table 4. The evaluation index of many object optimization methods.

No.	Measures	Formulation	Reference
1	Uniformity measure	$U = 1 - 2 \times (k - 1) \times \frac{\sum_{j=1}^{d} \sum_{i \in R_j} (f_i - \mu_j)^2}{N \times (f2min_{max}}$	[54]
2	Peak Signal-to-Noise Ratio (PSNR)	$PSNR = 10 \times log_{10}(\frac{255^2}{MSE})$ $MSE = \frac{1}{mn} \sum_{i=1}^{m-1} \sum_{j=1}^{n-1} [I(i,j) - K(i,j)]^2$	[55]
3	Feature Similarity Index (FSIM)	$FSIM = \frac{\sum_{x=\eta} S_L(x) \cdot PC_m(x)}{\sum_{x=\eta} PC_m(x)}$	[56]

Table 5. The FSIM of the comparison algorithms.

Image	K	EOA-Otsu	EOA-3DOtsu	HEOA-Otsu	HEOA-3DOtsu
Test1	4	0.8628	0.8886	0.8973	**0.9106**
	8	0.8657	0.8864	0.8957	**0.9170**
	12	0.9103	0.9332	0.9411	**0.9580**
	15	0.9293	0.9479	0.9565	**0.9695**
Test2	4	0.8644	0.8799	0.8901	**0.9015**

	8	0.8459	0.8674	0.8736	**0.9135**
	12	0.9298	0.9511	0.9569	**0.9591**
	15	0.9287	0.9474	0.9562	**0.9671**
Test3	4	0.8586	0.8833	0.8919	**0.9056**
	8	0.8599	0.8766	0.8859	**0.9246**
	12	0.9207	0.9370	0.9466	**0.9661**
	15	0.9049	0.9239	0.9358	**0.9688**
Test4	4	0.8518	0.8660	0.8805	**0.8963**
	8	0.8856	0.9060	0.9125	**0.9221**
	12	0.8823	0.9034	0.9143	**0.9619**
	15	0.9012	0.9260	0.9343	**0.9742**
Test5	4	0.8379	0.8545	0.8645	**0.8988**
	8	0.8648	0.8854	0.8992	**0.9193**
	12	0.9166	0.9305	0.9446	**0.9659**
	15	0.9055	0.9286	0.9345	**0.9750**
Test6	4	0.8725	0.8902	0.9025	**0.9157**
	8	0.8854	0.9040	0.9160	**0.9189**
	12	0.9267	0.9484	0.9566	**0.9585**
	15	0.8904	0.9095	0.9214	**0.9663**
Test7	4	0.8708	0.8883	0.9009	**0.9147**
	8	0.8845	0.9037	0.9155	**0.9171**
	12	0.9250	0.9478	0.9555	**0.9581**
	15	0.8898	0.9087	0.9202	**0.9648**
Test8	4	0.8704	0.8871	0.9000	**0.9143**
	8	0.8830	0.9017	0.9142	**0.9155**
	12	0.9232	0.9469	0.9535	**0.9578**
	15	0.8886	0.9079	0.9201	**0.9629**
Test9	4	0.8716	0.8884	0.9011	**0.9151**
	8	0.8844	0.9026	0.9157	**0.9163**
	12	0.9237	0.9470	0.9552	**0.9596**
	15	0.8897	0.9082	0.9217	**0.9633**
Test10	4	0.8720	0.8896	0.9024	**0.9171**
	8	0.8863	0.9027	0.9162	**0.9179**
	12	0.9247	0.9482	0.9561	**0.9607**
	15	0.8915	0.9089	0.9223	**0.9645**

4.1. HEOA optimize Otsu and 3DOtsu function

In this section, we compare the different segmentation method as fitness function. The EOA and HEOA optimize Otsu and 3DOtsu function. The FSIM of the compared algorithms can be seen from table 5. The Bar chart of the FSIM can be seen in Figure 6.

It can be seen from table 5, the FSIM value of 3DOtsu is better than Otsu. The 3DOtsu can use the information of color image, and get the best segment result. And the result of HEOA is better than EOA, it means that the Hybrid algorithm improves the optimal ability of EOA and makes the algorithm find the best result. Above analyze, we use the 3DOtsu as the fitness function in the next experiment.

The Figure 6 show the FSIM result of the compared algorithms. The result of 3DOtsu is better than the result of Otsu. The 3DOtsu use the information of three channels and obtains the better threshold than Otsu. At the same time, the result of HEOA is better than EOA, it means that the GOA can improve the optimal ability of the EOA.

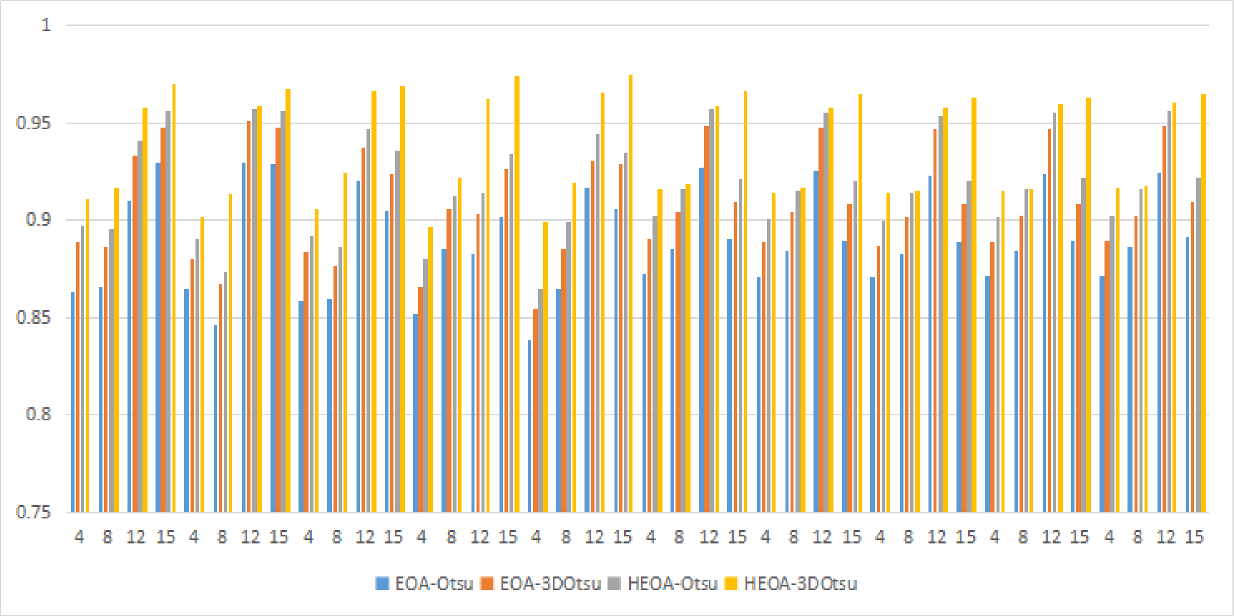

Figure 6. The FSIM result of compared algorithms.

4.2. Comparison with optimization algorithm based 3DOtsu

In this experiment, to show the merits of proposed technique, the results are compared with CSA, FPA, PSO, BA, HSOA [57] and HWOA [58] using 3DOtsu objective function. The parameters of the compared algorithms are set in the references.

The Figure 7 show the curve of Uniformity. It can be seen from figure, the HEOA obtains the best result in compared algorithms, the HSOA and HWOA gets the better result in compared algorithms, the CSA, FPA, PSO and BA obtains the worst result in all cases. It can be kwon that the hybrid optimization algorithms have the better optimal ability than original optimization algorithm. Most of all, the HEOA has the strongest ability in the compared algorithms.

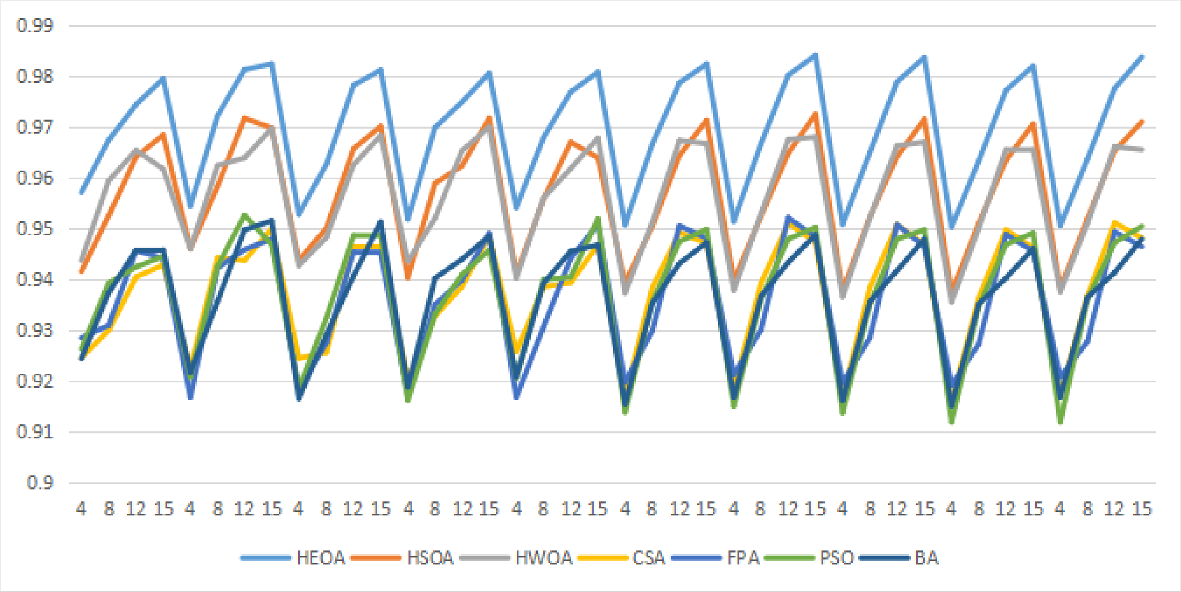

Figure 7. The Uniformity result of compared algorithms.

From Table 6, it can be observed that for all the test images, HEOA is better and more reliable than CSA, FPA, PSO, and BA, because of its precise search capability, at a high threshold level (K). Performance of HSOA and HWOA has closely followed HEOA. The solution update strategy for FPA and PSO may have led to poor results. The comprehensive performance ranking of the comparison algorithm is as follows: HEOA>HSOA>HWOA>PSO>BA>CSA> FPA. So, the HEOA have a better performance than other algorithms.

Table 7 and table 8 are PSNR and FSIM values of each algorithm respectively. As can be seen from the table, with the increase of the number of threshold values, the PSNR and FSIM values of the image have been significantly improved, indicating that the increase of the number of threshold values significantly improves the segmentation accuracy. The PSNR value of HEOA algorithm is better than other algorithms in all of the 24 groups. So, HEOA have a good competitive than other algorithms. Among all the data of FSIM, HEOA show an improvement of 1.42%, 1.35%, 4.21%, 4.02%, 4.19% and 4.09% over HSOA, HWOA, CSA, FPA, PSO and BA. This means that the segmentation results of HWOA are closer to the original image than other comparison algorithms.

Table 9 shows the CPU time of each algorithm under different thresholds. When the threshold value K = 4, the results of each optimization algorithm differ little. At this point, the number of thresholds is small, the search space is small, and the optimization capability of each optimization algorithm is basically the same. When K=15, the computational complexity of image segmentation increases and the CPU time increases absolutely. The average time of each algorithm in the test image is: HEOA < HSOA < HWOA < FPA < CSA < BA < PSO. So, the HEOA algorithm not only has the good performance in image segmentation, but also has the less CPU time than other compared algorithms.

Table 6. The Uniformity measure for the comparison algorithms.

Image	K	HEOA	HSOA	HWOA	CSA	FPA	PSO	BA
Test1	4	**0.9571**	0.9415	0.9437	0.9245	0.9284	0.9262	0.9243
	8	**0.9674**	0.9525	0.9594	0.9299	0.9309	0.9392	0.9373
	12	**0.9744**	0.9641	0.9654	0.9404	0.9456	0.9424	0.9457
	15	**0.9795**	0.9684	0.9617	0.9428	0.9441	0.9445	0.9458
Test2	4	**0.9544**	0.9460	0.9460	0.9224	0.9167	0.9207	0.9216
	8	**0.9722**	0.9583	0.9624	0.9442	0.9422	0.9425	0.9356
	12	**0.9813**	0.9717	0.9639	0.9437	0.9458	0.9526	0.9497
	15	**0.9824**	0.9698	0.9697	0.9499	0.9479	0.9468	0.9515
Test3	4	**0.9528**	0.9437	0.9427	0.9244	0.9184	0.9184	0.9165
	8	**0.9626**	0.9500	0.9482	0.9255	0.9274	0.9323	0.9290
	12	**0.9782**	0.9657	0.9625	0.9464	0.9453	0.9486	0.9406
	15	**0.9812**	0.9701	0.9683	0.9467	0.9450	0.9487	0.9513
Test4	4	**0.9518**	0.9403	0.9435	0.9201	0.9171	0.9161	0.9187
	8	**0.9699**	0.9589	0.9520	0.9327	0.9350	0.9331	0.9402
	12	**0.9749**	0.9623	0.9653	0.9385	0.9398	0.9409	0.9439
	15	**0.9806**	0.9717	0.9700	0.9486	0.9490	0.9457	0.9485
Test5	4	**0.9541**	0.9410	0.9402	0.9257	0.9167	0.9206	0.9207
	8	**0.9679**	0.9558	0.9560	0.9385	0.9306	0.9399	0.9392
	12	**0.9769**	0.9670	0.9618	0.9393	0.9441	0.9404	0.9455
	15	**0.9808**	0.9639	0.9678	0.9468	0.9508	0.9519	0.9467
Test6	4	**0.9507**	0.9393	0.9373	0.9169	0.9197	0.9138	0.9154
	8	**0.9666**	0.9504	0.9512	0.9383	0.9298	0.9355	0.9352
	12	**0.9787**	0.9644	0.9673	0.9492	0.9505	0.9474	0.9431
	15	**0.9824**	0.9713	0.9667	0.9470	0.9480	0.9498	0.9472
Test7	4	**0.9514**	0.9397	0.9378	0.9183	0.9212	0.9150	0.9167
	8	**0.9667**	0.9524	0.9529	0.9392	0.9300	0.9360	0.9366
	12	**0.9802**	0.9648	0.9675	0.9510	0.9521	0.9479	0.9433
	15	**0.9841**	0.9725	0.9680	0.9473	0.9483	0.9502	0.9487
Test8	4	**0.9508**	0.9377	0.9365	0.9165	0.9196	0.9137	0.9161
	8	**0.9649**	0.9522	0.9520	0.9383	0.9284	0.9349	0.9355
	12	**0.9789**	0.9642	0.9663	0.9507	0.9507	0.9479	0.9417
	15	**0.9837**	0.9715	0.9670	0.9468	0.9464	0.9497	0.9479
Test9	4	**0.9503**	0.9374	0.9355	0.9158	0.9191	0.9118	0.9151
	8	**0.9633**	0.9510	0.9500	0.9363	0.9272	0.9346	0.9351
	12	**0.9772**	0.9634	0.9655	0.9497	0.9488	0.9468	0.9402
	15	**0.9820**	0.9706	0.9655	0.9462	0.9455	0.9491	0.9460
Test10	4	**0.9505**	0.9382	0.9375	0.9171	0.9207	0.9118	0.9167
	8	**0.9637**	0.9519	0.9510	0.9367	0.9277	0.9360	0.9364
	12	**0.9776**	0.9653	0.9661	0.9511	0.9493	0.9472	0.9413
	15	**0.9838**	0.9710	0.9655	0.9481	0.9464	0.9504	0.9479

Table 7. The PSNR for the comparison algorithms.

Image	K	HEOA	HSOA	HWOA	CSA	FPA	PSO	BA
Test1	4	**23.3863**	23.2573	23.2526	23.0420	23.0405	23.0397	23.0539
	8	**29.2231**	29.1025	29.0968	28.9021	28.9007	28.8989	28.9020
	12	**32.5692**	32.4393	32.4442	32.2300	32.2265	32.2282	32.2414
	15	**33.3295**	33.1947	33.1953	33.0002	32.9903	32.9903	32.9923
Test2	4	**24.4702**	24.3443	24.3386	24.1472	24.1340	24.1342	24.1432
	8	**29.4260**	29.3020	29.2936	29.0852	29.0987	29.0861	29.1020
	12	**32.5786**	32.4454	32.4470	32.2471	32.2464	32.2522	32.2424
	15	**34.2153**	34.0865	34.0884	33.8828	33.8824	33.8823	33.8887
Test3	4	**24.4769**	24.3474	24.3453	24.1433	24.1406	24.1517	24.1495
	8	**29.9667**	29.8287	29.8366	29.6330	29.6383	29.6298	29.6211
	12	**32.6661**	32.5412	32.5392	32.3369	32.3265	32.3288	32.3254
	15	**34.7330**	34.6031	34.6015	34.3994	34.3925	34.4084	34.3905
Test4	4	**24.7640**	24.6386	24.6369	24.4284	24.4400	24.4423	24.4286
	8	**29.5467**	29.4208	29.4154	29.2214	29.2193	29.2207	29.2104
	12	**33.5823**	33.4474	33.4548	33.2561	33.2435	33.2461	33.2509
	15	**34.2159**	34.0826	34.0820	33.8787	33.8740	33.8707	33.8853
Test5	4	**24.5319**	24.3991	24.3994	24.2048	24.1918	24.1918	24.1924
	8	**29.5550**	29.4198	29.4251	29.2137	29.2181	29.2237	29.2154
	12	**34.3322**	34.1972	34.1979	34.0010	33.9935	33.9870	33.9959
	15	**35.0669**	34.9409	34.9366	34.7387	34.7254	34.7407	34.7279
Test6	4	**25.2119**	25.0871	25.0842	24.8695	24.8803	24.8734	24.8829
	8	**30.9087**	30.7880	30.7821	30.5869	30.5821	30.5735	30.5700
	12	**34.1912**	34.0606	34.0591	33.8576	33.8505	33.8585	33.8626
	15	**35.7843**	35.6567	35.6607	35.4492	35.4505	35.4438	35.4423
Test7	4	**25.4053**	25.1458	25.1450	24.8847	25.0748	24.9284	24.9402
	8	**31.0914**	30.8883	30.8601	30.7788	30.5828	30.6162	30.6718
	12	**34.3507**	34.1142	34.1742	34.0164	33.9942	33.8766	33.8983
	15	**35.9362**	35.6969	35.7545	35.6007	35.4588	35.4937	35.6024
Test8	4	**25.5670**	25.2034	25.2799	24.9384	25.1283	24.9787	25.0445
	8	**31.2698**	31.0054	30.9921	30.8672	30.7368	30.6972	30.8372
	12	**34.5283**	34.2658	34.2137	34.2017	34.1031	33.9285	34.0632
	15	**36.0846**	35.7585	35.9118	35.6393	35.6021	35.4988	35.6352
Test9	4	**25.5622**	25.0597	25.1265	24.7749	24.9583	24.9368	24.8720
	8	**31.1656**	30.8841	30.8166	30.7155	30.6732	30.6568	30.8154
	12	**34.4249**	34.0884	34.1830	34.1183	33.9539	33.7553	33.9067
	15	**36.0382**	35.7553	35.7737	35.5952	35.5146	35.3593	35.5413
Test10	4	**25.4424**	24.9891	25.1108	24.7329	24.7752	24.9286	24.8300
	8	**31.1315**	30.7681	30.7427	30.5414	30.6599	30.5129	30.6245
	12	**34.3961**	33.9364	34.1416	33.9835	33.8675	33.7435	33.8129
	15	**35.8866**	35.7225	35.7457	35.4554	35.4165	35.2905	35.3448

Table 8. The FSIM for the comparison algorithms.

Image	K	HEOA	HSOA	HWOA	CSA	FPA	PSO	BA
Test1	4	**0.9367**	0.9236	0.9225	0.9094	0.9039	0.8944	0.9087
	8	**0.9517**	0.9414	0.9390	0.9036	0.9077	0.9157	0.9084
	12	**0.9587**	0.9433	0.9473	0.9135	0.9149	0.9172	0.9135
	15	**0.9668**	0.9511	0.9540	0.9271	0.9331	0.9287	0.9284
Test2	4	**0.9356**	0.9227	0.9262	0.9006	0.8943	0.8936	0.9065
	8	**0.9584**	0.9422	0.9438	0.9221	0.9123	0.9122	0.9230
	12	**0.9632**	0.9548	0.9563	0.9283	0.9305	0.9331	0.9233
	15	**0.9633**	0.9553	0.9506	0.9242	0.9251	0.9255	0.9202
Test3	4	**0.9325**	0.9197	0.9181	0.9003	0.9077	0.8898	0.9078
	8	**0.9477**	0.9333	0.9362	0.9060	0.9062	0.9001	0.9048
	12	**0.9599**	0.9482	0.9483	0.9289	0.9289	0.9190	0.9162
	15	**0.9607**	0.9487	0.9468	0.9309	0.9251	0.9325	0.9358
Test4	4	**0.9385**	0.9213	0.9207	0.9065	0.9063	0.8982	0.8954
	8	**0.9485**	0.9362	0.9349	0.9057	0.9058	0.9115	0.9144
	12	**0.9580**	0.9487	0.9498	0.9240	0.9298	0.9154	0.9200
	15	**0.9637**	0.9457	0.9532	0.9229	0.9227	0.9321	0.9237
Test5	4	**0.9332**	0.9213	0.9264	0.8894	0.9071	0.9082	0.8960
	8	**0.9469**	0.9377	0.9361	0.9085	0.9141	0.9083	0.9106
	12	**0.9642**	0.9438	0.9503	0.9210	0.9254	0.9187	0.9270
	15	**0.9687**	0.9484	0.9489	0.9240	0.9174	0.9240	0.9267
Test6	4	**0.9304**	0.9238	0.9186	0.8868	0.9055	0.8972	0.9054
	8	**0.9518**	0.9317	0.9372	0.9027	0.9099	0.9117	0.9085
	12	**0.9579**	0.9492	0.9460	0.9280	0.9270	0.9258	0.9158
	15	**0.9682**	0.9517	0.9490	0.9289	0.9204	0.9315	0.9250
Test7	4	**0.9313**	0.9252	0.9198	0.8882	0.9057	0.8984	0.9060
	8	**0.9536**	0.9322	0.9384	0.9035	0.9109	0.9127	0.9087
	12	**0.9590**	0.9498	0.9477	0.9287	0.9280	0.9273	0.9177
	15	**0.9699**	0.9524	0.9510	0.9292	0.9222	0.9335	0.9258
Test8	4	**0.9294**	0.9239	0.9181	0.8877	0.9044	0.8970	0.9058
	8	**0.9518**	0.9309	0.9381	0.9029	0.9096	0.9116	0.9070
	12	**0.9573**	0.9487	0.9470	0.9276	0.9263	0.9263	0.9175
	15	**0.9682**	0.9513	0.9494	0.9280	0.9216	0.9324	0.9240
Test9	4	**0.9292**	0.9234	0.9161	0.8866	0.9038	0.8956	0.9052
	8	**0.9506**	0.9296	0.9368	0.9010	0.9089	0.9096	0.9064
	12	**0.9569**	0.9469	0.9470	0.9273	0.9250	0.9262	0.9160
	15	**0.9676**	0.9501	0.9474	0.9275	0.9216	0.9308	0.9236
Test10	4	**0.9296**	0.9246	0.9170	0.8874	0.9046	0.8962	0.9057
	8	**0.9509**	0.9306	0.9378	0.9025	0.9093	0.9098	0.9069
	12	**0.9589**	0.9483	0.9490	0.9275	0.9261	0.9277	0.9165
	15	**0.9678**	0.9501	0.9479	0.9287	0.9232	0.9316	0.9240

Table 9. The CPU time for the comparison algorithms.

Image	K	HEOA	HSOA	HWOA	CSA	FPA	PSO	BA
Test1	4	**1.2145**	1.2251	1.2247	1.2442	1.2405	1.2406	1.2389
	8	**1.3154**	1.3254	1.3260	1.3452	1.3422	1.3386	1.3385
	12	**1.5172**	1.5274	1.5279	1.5448	1.5467	1.5451	1.5466
	15	**1.8157**	1.8260	1.8258	1.8359	1.8435	1.8376	1.8439
Test2	4	**1.2149**	1.2259	1.2255	1.2363	1.2392	1.2436	1.2365
	8	**1.3154**	1.3262	1.3263	1.3388	1.3411	1.3401	1.3371
	12	**1.5181**	1.5286	1.5288	1.5423	1.5449	1.5466	1.5389
	15	**1.8158**	1.8266	1.8266	1.8419	1.8398	1.8409	1.8424
Test3	4	**1.2151**	1.2257	1.2258	1.2354	1.2367	1.2445	1.2367
	8	**1.3158**	1.3268	1.3265	1.3402	1.3411	1.3456	1.3436
	12	**1.5191**	1.5292	1.5292	1.5394	1.5406	1.5474	1.5487
	15	**1.8164**	1.8270	1.8273	1.8462	1.8369	1.8437	1.8413
Test4	4	**1.2151**	1.2254	1.2253	1.2444	1.2358	1.2358	1.2409
	8	**1.3166**	1.3268	1.3271	1.3432	1.3398	1.3458	1.3461
	12	**1.5192**	1.5299	1.5301	1.5421	1.5476	1.5483	1.5465
	15	**1.8166**	1.8275	1.8269	1.8390	1.8466	1.8422	1.8425
Test5	4	**1.2161**	1.2269	1.2269	1.2388	1.2447	1.2368	1.2401
	8	**1.3167**	1.3273	1.3273	1.3456	1.3396	1.3382	1.3431
	12	**1.5201**	1.5304	1.5302	1.5471	1.5428	1.5454	1.5401
	15	**1.8169**	1.8274	1.8278	1.8431	1.8379	1.8456	1.8405
Test6	4	**1.2168**	1.2271	1.2268	1.2372	1.2413	1.2412	1.2383
	8	**1.3172**	1.3281	1.3273	1.3412	1.3407	1.3448	1.3379
	12	**1.5206**	1.5307	1.5313	1.5491	1.5408	1.5445	1.5493
	15	**1.8169**	1.8278	1.8270	1.8395	1.8463	1.8410	1.8428
Test7	4	**1.2183**	1.2275	1.2282	1.2373	1.2421	1.2429	1.2399
	8	**1.3179**	1.3284	1.3291	1.3429	1.3420	1.3463	1.3391
	12	**1.5219**	1.5326	1.5316	1.5510	1.5410	1.5462	1.5506
	15	**1.8179**	1.8293	1.8289	1.8408	1.8466	1.8410	1.8440
Test8	4	**1.2173**	1.2270	1.2272	1.2371	1.2403	1.2424	1.2393
	8	**1.3167**	1.3278	1.3282	1.3409	1.3401	1.3447	1.3386
	12	**1.5217**	1.5308	1.5303	1.5497	1.5398	1.5460	1.5498
	15	**1.8172**	1.8273	1.8284	1.8396	1.8446	1.8397	1.8424
Test9	4	**1.2154**	1.2265	1.2258	1.2357	1.2391	1.2409	1.2376
	8	**1.3166**	1.3268	1.3277	1.3398	1.3389	1.3428	1.3375
	12	**1.5204**	1.5304	1.5291	1.5482	1.5397	1.5453	1.5485
	15	**1.8154**	1.8272	1.8281	1.8395	1.8431	1.8385	1.8422
Test10	4	**1.2155**	1.2282	1.2270	1.2377	1.2404	1.2419	1.2380
	8	**1.3172**	1.3283	1.3279	1.3401	1.3399	1.3444	1.3391
	12	**1.5207**	1.5319	1.5305	1.5494	1.5397	1.5460	1.5495
	15	**1.8160**	1.8272	1.8297	1.8400	1.8440	1.8393	1.8442

4.3. Statistical analysis

The experimental results of each algorithm are the same, so statistical tests are needed. Parametric statistical tests are based on various assumptions [59]. The well-known non-parametric statistical tests, namely Friedman test [60] and Wilcoxon rank-sum test [61] are used in this section. For the average rank of Friedman's test given in table 10, the method presented in this paper takes the first place in all cases, and as the number of threshold levels increases, the rank value becomes smaller and smaller, which has greater advantages compared with other comparison methods. Through the above analysis, as the dimension of optimization problem increases, the optimization ability of the proposed algorithm HEOA becomes more and more obvious.

Table 10. Results of Friedman rank test over all available test images.

K	HEOA	HSOA	HWOA	CSA	FPA	PSO	BA
4	**3.1581**	3.4458	3.5147	3.4581	3.6152	3.9951	3.8547
8	**2.9315**	3.5514	3.6891	3.5125	3.9156	3.9514	3.6984
12	**1.9984**	2.5589	3.6661	3.1285	3.9991	3.9541	3.8854
15	**1.7415**	2.6518	3.6581	3.1814	3.8147	3.8574	3.7781
Overall	**2.4574**	3.0520	3.6320	3.3201	3.8362	3.9395	3.8042

The experimental statistical results are shown in Table 11 below. The null hypothesis is constructed as: there is no significant difference between the two algorithms. The alternative hypothesis states that there is a significant difference between the two algorithms. In the experiment, HEOA based method produces better result in 36 out of 40 cases when compared with HSOA based method and produces better result in 35 out of 40 cases when compared with HWOA based method and produces better result in 38 out of 40 cases when compared with CSA based method and produces better result in 38 out of 40 cases when compared with FPA based method and produces better result in 40 out of 40 cases when compared with the PSO based method. As can be seen from the results, there are significant differences among the six algorithms. In most cases, HEOA performs better than other algorithms.

4.4. Compared with novel image segmentation method using wood fiber images

In this section, we compare with the novel image segmentation methods. The compared algorithms are PCNN [62], fuzzy c-means (FCM) [63], grayscale co-occurrence matrix (GLCM) [64]. In order to test the performance of the color image segmentation algorithms, we select the wood fibers which are taken under a high-powered microscope as the test images. The figures 8–11 show the wood fiber images and the segmentation result.

It can be seen from the figures 4–7, the result of PCNN has the over-segmentation phenomenon and the segmented images are the worst of the compared algorithms. The FCM and GLCM have the under-segmentation phenomenon and the results of the fiber images are not clear. Among the result of the fiber images, the HEOA-3DOtsu get the best result. The table 12 shows the HEOS obtains a large improvement than the others compared image segmentation methods. The recall and precision are 93.19% and 91.28% respectively. The results show that the performance of this method can provide the segmentation result of the wood fiber image. The Figure12 show the segmentation result of the proposed method. It can be seen from figure, the number of wood fiber can be seen clearly. This method obtains independent wood fiber area. So, the proposed method can segment the wood fiber images successfully and have strong robustness.

Table 11. P-value of Wilcoxon test comparative Kapur based method**.**

Images	K	HSOA	HWOA	CSA	FPA	PSO
Test1	4	P<0.05	P<0.05	P<0.05	P<0.05	P<0.05
	8	P>0.05	P<0.05	P<0.05	P<0.05	P<0.05
	12	P<0.05	P<0.05	P<0.05	P<0.05	P<0.05
	15	P<0.05	P>0.05	P<0.05	P<0.05	P<0.05
Test2	4	P<0.05	P<0.05	P<0.05	P>0.05	P<0.05
	8	P<0.05	P<0.05	P<0.05	P<0.05	P<0.05
	12	P<0.05	P<0.05	P<0.05	P<0.05	P<0.05
	15	P<0.05	P<0.05	P<0.05	P<0.05	P<0.05
Test3	4	P<0.05	P<0.05	P<0.05	P<0.05	P<0.05
	8	P<0.05	P<0.05	P<0.05	P<0.05	P<0.05
	12	P<0.05	P<0.05	P<0.05	P<0.05	P<0.05
	15	P<0.05	P<0.05	P<0.05	P<0.05	P<0.05
Test4	4	P<0.05	P<0.05	P<0.05	P<0.05	P<0.05
	8	P>0.05	P<0.05	P<0.05	P<0.05	P<0.05
	12	P<0.05	P>0.05	P<0.05	P<0.05	P<0.05
	15	P<0.05	P<0.05	P<0.05	P<0.05	P<0.05
Test5	4	P<0.05	P<0.05	P<0.05	P<0.05	P<0.05
	8	P<0.05	P<0.05	P<0.05	P<0.05	P<0.05
	12	P<0.05	P<0.05	P<0.05	P<0.05	P<0.05
	15	P<0.05	P<0.05	P<0.05	P<0.05	P<0.05
Test6	4	P>0.05	P<0.05	P<0.05	P<0.05	P<0.05
	8	P<0.05	P<0.05	P<0.05	P<0.05	P<0.05
	12	P<0.05	P<0.05	P<0.05	P<0.05	P<0.05
	15	P<0.05	P<0.05	P<0.05	P<0.05	P<0.05
Test7	4	P<0.05	P<0.05	P>0.05	P<0.05	P<0.05
	8	P<0.05	P<0.05	P<0.05	P<0.05	P<0.05
	12	P<0.05	P<0.05	P<0.05	P<0.05	P<0.05
	15	P<0.05	P<0.05	P<0.05	P<0.05	P<0.05
Test8	4	P>0.05	P<0.05	P<0.05	P>0.05	P<0.05
	8	P<0.05	P>0.05	P<0.05	P<0.05	P<0.05
	12	P<0.05	P<0.05	P<0.05	P<0.05	P<0.05
	15	P<0.05	P<0.05	P<0.05	P<0.05	P<0.05
Test9	4	P<0.05	P<0.05	P<0.05	P<0.05	P<0.05
	8	P<0.05	P>0.05	P<0.05	P<0.05	P<0.05
	12	P<0.05	P<0.05	P<0.05	P<0.05	P<0.05
	15	P<0.05	P<0.05	P<0.05	P<0.05	P<0.05
Test10	4	P<0.05	P>0.05	P>0.05	P<0.05	P<0.05
	8	P<0.05	P<0.05	P<0.05	P<0.05	P<0.05
	12	P<0.05	P<0.05	P<0.05	P<0.05	P<0.05
	15	P<0.05	P<0.05	P<0.05	P<0.05	P<0.05

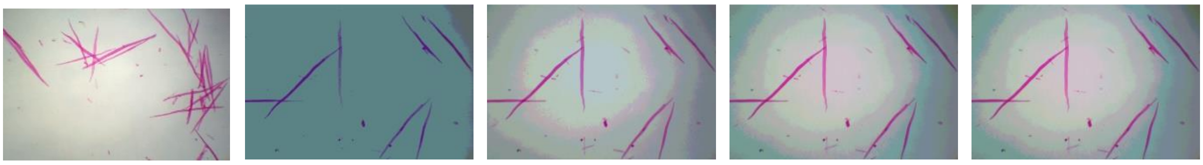
(a) fiber1 (b) PCNN (c) FCM (d) GLCM (e) HEOA-3DOtsu

Figure 8. The segmented result of wood fiber image1.

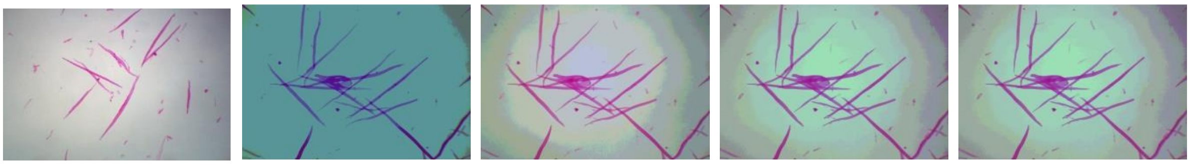
(a) fiber2 (b) PCNN (c) FCM (d) GLCM (e) HEOA-3DOtsu

Figure 9. The segmented result of wood fiber image2.

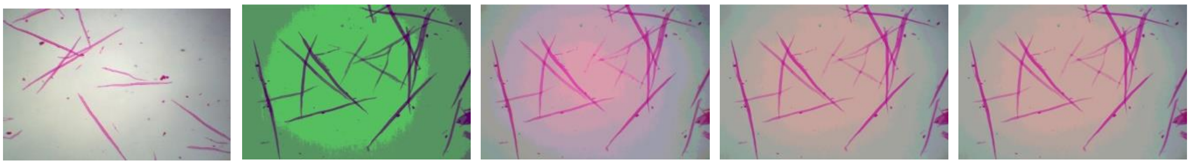
(a) fiber3 (b) PCNN (c) FCM (d) GLCM (e) HEOA-3DOtsu

Figure 10. The segmented result of wood fiber image3.

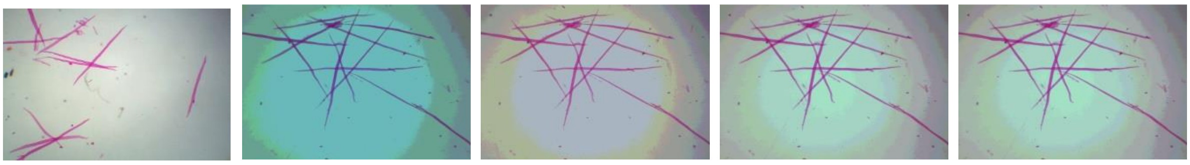
(a) fiber4 (b) PCNN (c) FCM (d) GLCM (e) HEOA-3DOtsu

Figure 11. The segmented result of wood fiber image4.

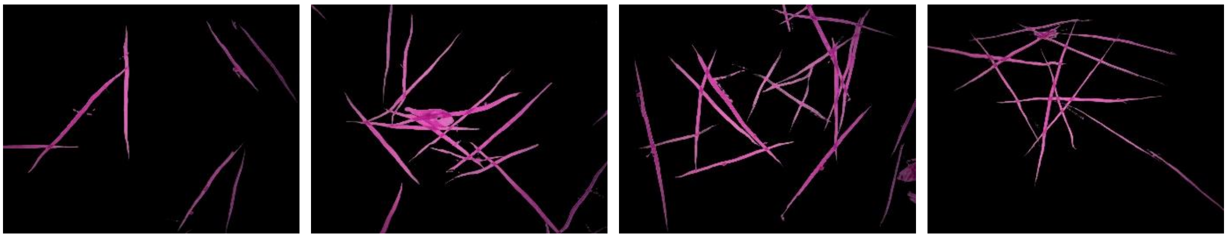
(a) fiber1 (b) fiber2 (c)fiber3 (d)fiber4

Figure 12. The segmented result of HEOA-3DOtus.

Table 12. Segmentation accuracy of compared image segmentation methods.

Method	R (%)	P (%)	AP (%)	VAL (%)
FCM	84.94	90.88	91.23	88.47
PCNN	80.46	90.69	81.46	79.46
DLA	70.12	92.95	78.32	77.57
BMPA	**93.19**	**91.28**	91.45	90.38

5. Discussion

The analysis of wood fiber graphics can understand the state of the fiber, so as to ensure the production of wood or paper that meets industrial requirements. The scholar Mainly analyze the shape and thickness of individual wood fibers. However, the wood fibers in the collected graphics are more responsible and similar to the background. Traditional segmentation methods cannot solve this problem. So, study the novel image segmentation method is necessary.

In the field of optimization algorithm, the proposed method has a good optimal ability solve the CEC2015. And the proposed method has a good competitiveness with the CSA, FPA, PSO, BA and basic EOA. Because of the hybrid optimization algorithm use the advantage of the two optimization algorithms to optimize the complex benchmark function. At the same time, the proposed method solves the threshold image segmentation and find the best threshold from the 3DOtsu. The algorithm gets the best result among CSA, FPA, PSO, BA, HSOA and HWOA. The hybrid optimization algorithms enhance the optimal ability of the original optimization algorithm.

In the field of the fiber wood image segmentation, the proposed method obtains the highest segmentation accuracy with PCNN, FCN and GLCM. The PCNN obtains the worst result in compared algorithms, the performance of PCNN rely on the set of parameters. The FCN and GLCM has strong ability to solve the grey image, however, these two methods take huge challenge to segment color image. The proposed method can overcome the difficult of color image. Finally, the proposed method obtains the wood fiber area exactly.

The limitations of the proposed method can be divided in two contents. First, similar to other optimization algorithms, this algorithm takes time to iterate to find the best solution, which is time-consuming. Second, this method has strong performance in the field of wood fiber image segmentation. In order to make the proposed method can adopt more real area, we will study the novel optimization algorithm.

The proposed method can solve the other problem of optimization. At the same time, it can be used in the field of medical image segmentation, forest fire image segmentation and so on. In the future, we will continue to study many object multi-level threshold methods and different optimization algorithms, so as to improve the image segmentation accuracy.

6. Conclusions

In this paper, the HEOA algorithm is used to optimize the 3DOtsu algorithm to obtain the optimal multi-threshold image. We use GOA to improve EOA algorithm and enhance the optimization ability of the algorithm. The CEC2015 is selected as benchmark function to test the performance of the hybrid optimization algorithms. The result shows that the hybrid algorithm can enhance the optimal ability of the EOA. And then, the HEOA is compared with other optimization algorithms to jointly optimize

3DOtsu algorithm for classic images and wood fiber images segmentation experiments. From U measure, PSNR and FSIM values, it can be seen that 3DOtsu-HEOA algorithm has the best segmentation accuracy. Finally, we compare the 3DOtsu-HEOA algorithm with the novel image segmentation method. It can be seen from the segmented result that HEOA can get the best segmented result. So, the 3DOtsu-HEOA algorithm proposed in this paper has better image segmentation accuracy and better stability.

Acknowledgements

This work was supported by the Fundamental Research Funds for the Central Universities under Grant No. 2572018BH08.

Conflict of interest

The authors have no conflict of interest.

References

1. Y. Li, X. Bai, L. Jiao, Y. Xue, Partitioned-cooperative quantum-behaved particle swarm optimization based on multilevel thresholding applied to medical image segmentation, *Appl. Soft Comput.*, **56** (2017), 345–356.
2. M. A. E. Aziz, A. A. Ewees, A. E. Hassanien, Whale Optimization Algorithm and Moth-Flame Optimization for multilevel thresholding image segmentation, *Expert Syst. Appl.*, **83** (2017), 242–256.
3. B. Leszczyński, A. Gancarczyk, A. Wróbel, M. Piatek, J. Lojewska, A. Kolodziej, et al., Global and local thresholding methods applied to X-ray microtomographic analysis of Metallic Foams, *J. Nondestruct. Eval.*, **35** (2016), 35–35.
4. K. Somkantha, N. Theera-Umpon, S. Auephanwiriyakul, Boundary detection in medical images using edge following algorithm based on intensity gradient and texture gradient features, *IEEE Trans. Biomed. Eng.*, **58** (2011), 567–573.
5. T. H. Farag, W. A. Hassan, H. A. Ayad, A. S. AlBahussain, U. A. Badawi, M. K. Alsmadi, Extended absolute fuzzy connectedness segmentation algorithm utilizing region and boundary-based information, *Arab. J. Sci. Eng.*, **42** (2017), 3573–3583.
6. S. Niu, C. Qiang, L. D. Sisternes, Z. Ji, Z. Zhou, D. Rubin, Robust noise region-based active contour model via local similarity factor for image segmentation, *Pattern Recognit.*, **61** (2017), 104–119.
7. L. Fan, D. A. Clausi, L. Xu, A. Wong, ST-IRGS: A region-based self-training algorithm applied to hyperspectral image classification and segmentation, *IEEE Trans. Geosci. Remote Sensing*, **56** (2018), 3–16.
8. X. Cheng, C. M. Shuai, J. Wang, W. Li, J. Shuai, Y. Liu, Building a sustainable development model for China's poverty-stricken reservoir regions based on system dynamics, *J. Clean Prod.*, **176** (2018), 535–554.
9. S. Dong, H. Li, J. Wang, X. Zhang, X. Ji, Improved flexible Li-ion hybrid capacitors: Techniques for superior stability, *Nano Res.*, **10** (2017), 4448–4456.
10. K. S. Hong, M. J. Khan, Hybrid brain–computer interface techniques for improved classification accuracy and increased number of commands: A review, *Front. Neurorobot.*, **11** (2017), 35.

11. T. Lv, G. Yang, Y. Zhang, Y. Zhang, J. Yang, Y. Chen, Vessel segmentation using centerline constrained level set method, *Multimed. Tools Appl.*, **78** (2019), 17051–17075.
12. Y. Chen, Y. Zhang, J. Yang, Curve-like structure extraction using minimal path propagation with backtracing, *IEEE Trans. Image Process*, **25** (2016), 988–1003.
13. L. Ngo, J. Cha, J. H. Han, Deep neural network regression for automated retinal layer segmentation in optical coherence tomography images, *IEEE Trans. Image Process*, **29** (2020), 303–312.
14. C. Guan, S. Wang, W. C. Liew, Lip image segmentation based on a fuzzy convolutional neural network, *IEEE Trans. Fuzzy Syst.*, **28** (2019), 1242–1251.
15. A. M. Bensaid, L. Hal, J. Bezdek, L. Clarke, M. Silbiger, J. Arrington, R. Murtagh, Validity-guided (re)clustering with applications to image segmentation, *IEEE Trans. Fuzzy Syst.*, **4** (1996), 112–123.
16. N. Otsu, A threshold selection method from gray-level histograms, *IEEE Trans. Syst. Man. Cybern. -Syst.*, **9** (2007), 62–66.
17. W. Hussein, S. Sahran, S. Abdullah, A fast scheme for multilevel thresholding based on a modified bees algorithm, *Knowledge-Based Syst.*, **101** (2016), 114–134.
18. J. Liu, W. Li, Y. Tian, Automatic thresholding of gray-level pictures using two-dimension Otsu method, *1991 International Conference on Circuits and Systems*, (1991), 325–327.
19. X. J. Jing, J. F. Li, Y. L. Liu, Image segmentation based on 3-D maximum between-cluster variance, Acta Elect, *Acta. Electronica. Sinica.*, **31** (2003), 1281–1285.
20. L. Wang, H. Duan, J. Wang, A fast algorithm for three-dimensional Otsu's thresholding method, *2008 IEEE International Symposium on IT in Medicine and Education*, *IEEE*, 2008, 136–140.
21. L. Bian, G. Huo, Q. Li, Multi-threshold MRI image segmentation algorithm based on Curevelet transformation and multi-objective particle swarm optimization, *J. Comp. Appl.*, **36** (2016), 3188–3195.
22. N. Muangkote, K. Sunat, S. Chiewchanwattana, Multilevel thresholding for satellite image segmentation with moth-flame based optimization, *International Joint Conference on Computer Science & Software Engineering*, *IEEE*, (2016).
23. S. Borjigin, P. Sahoo, Color Image Segmentation based on multi-level Tsallis-Havrda-Charvát entropy and 2D histogram using PSO Algorithms, *Pattern Recognit.*, **92** (2019), 107–118.
24. A. Wunnava, M. Naik, R. Panda, B. Jena, A. Abraham, An adaptive Harris hawks optimization technique for two dimensional grey gradient based multilevel image thresholding, *Appl. Soft Comput.*, **95** (2020), 106526.
25. A. Bhandari, K. Rahul, A context sensitive Masi entropy for multilevel image segmentation using moth swarm algorithm, *Infrared Phys. Technol.*, **98** (2019), 132–154.
26. A. Koshki, M. Zekri, R. Ahmadzadeh, S. Sadri, E. Mahmoudzadeh, Extending contour level set model for multi-class image segmentation with Application to Breast Thermography Images, *Infrared Phys. Technol.*, **105** (2020), 103174.
27. D. Yousri, M. A. Elaziz, S. Mirjalili, Fractional-order calculus-based flower pollination algorithm with local search for global optimization and image segmentation, *Knowledge-Based Syst.*, **197** (2020), 105889–105894.
28. M. Marinaki, Y. Marinakis, A glowworm swarm optimization algorithm for the vehicle routing problem with stochastic demands, *Expert Syst. Appl.*, **46** (2016), 145–163.
29. H. Bouchekara, A. Chaib, M. Abido, R. Sehiemy, Optimal power flow using an Improved Colliding Bodies Optimization algorithm, *Appl. Soft Comput.*, **42** (2016), 119–131.
30. A. E. Smith, Multi-objective optimization using evolutionary algorithms, *IEEE Trans. Evol. Comput.*, **6** (2002), 526–526.

31. D. E. Goldberg, J. H. Holland, Genetic algorithms and machine learning, *Mach. Learn.*, **3** (1988), 95–99.
32. R. Storn, K. Price, Differential evolution—A simple and efficient heuristic for global optimization over continuous spaces, *J. Glob. Optim.*, **11** (1997), 341–359.
33. J. Kennedy, R. Eberhart, Particle swarm optimization, *Proceedings of ICNN'95—International Conference on Neural Networks*, *IEEE*, 2002.
34. M. Seyedali, The Ant Lion Optimizer, *Adv. Eng. Softw.*, **83** (2015), 80–98.
35. A. Askarzadeh, A novel metaheuristic method for solving constrained engineering optimization problems: Crow search algorithm, *Comput. Struct.*, **169** (2016), 1–12.
36. T. Biyanto, Matradji, S. Irawan, H. Febrianto, N. Afdanny, A. Rahman, et al, Killer Whale algorithm: An algorithm inspired by the life of Killer Whale, *Proced. Computer Sci.*, **124** (2017), 151–157.
37. Z. Geem, J. H. Kim, G. V. Loganathan, A new heuristic optimization algorithm: Harmony search, *Simulation*, **76** (2001), 60–68.
38. Y. Zheng, Water wave optimization: A new nature-inspired metaheuristic, *Comput. Oper. Res.*, **55** (2015), 1–11.
39. A. Faramarzi, M. Heidarinejad, B. Strphens, S. Mirjalili, Equilibrium optimizer algorithm: A novel meta-heuristic optimization algorithm, *Adv. Eng. Softw*are, **191** (2020), 105190.
40. D. H. Wolpert, W. G. Macready, No free lunch theorems for optimization, *IEEE Trans. Evol. Comput.*, **1** (1997), 67–82.
41. H. Xu, W. Liang, Q. Gao, A self-gap-correction method for accurate permittivity measurement using the hybrid optimization algorithm, *IEEE Trans. Instrum. Meas.*, **68** (2019), 1781–1787.
42. P. Upadhyay, J. K. Chhabra, Multilevel thresholding based image segmentation using new multistage hybrid optimization algorithm, *J. Ambient Intell. Humaniz. Comput.*, **12** (2021), 1081–1098.
43. A. Kaur, C. Singh, SAR image segmentation based on hybrid PSOGSA optimization algorithm, *Int. J. Eng. Res. Appl.*, **4** (2014), 5–11.
44. D. Kole, A. Halder, An efficient dynamic image segmentation algorithm using a hybrid technique based on particle swarm optimization and genetic algorithm, *International Conference on Advances in Computer Engineering*, *IEEE*, 2010.
45. H. Gao, C. M. Pun, S. Kwong, An efficient image segmentation method based on a hybrid particle swarm algorithm with learning strategy, *Inf. Sci.*, **369** (2016), 500–521.
46. M. H. Mozaffari, W. S. Lee, Convergent heterogeneous particle swarm optimisation algorithm for multilevel image thresholding segmentation, *IET Image Process.*, **11** (2017), 605–619.
47. A. Bhandari, I.V. Kumar, K. Srinivas, Cuttlefish Algorithm-Based Multilevel 3-D Otsu Function for Color Image Segmentation, *IEEE Trans. Instrum. Meas.*, **69** (2020), 1871–1880.
48. S. Saremi, S. Mirjalili, A. Lewis, Grasshopper optimisation algorithm: Theory and application, *Adv. Eng. Softw.*, **105** (2017), 30–47.
49. Y. Sun, J. Wei, T. Wu, K. Xiao, J. Bao, Y. Jin, Brain storm optimization using a slight relaxation selection and multi-population based creating ideas ensemble, *Appl. Intell.*, **50** (2020), 3137–3161.
50. D. Oliva, S. Hinojosa, E. Cuevas, G. Pajares, O. Avalos, J. Gálvez, Cross entropy based thresholding for magnetic resonance brain images using Crow Search Algorithm, *Expert Syst. Appl.*, **79** (2017), 164–180.

51. A. Y. Abdelaziz, E. S. Ali, S. A. Elazim, Implementation of flower pollination algorithm for solving economic load dispatch and combined economic emission dispatch problems in power systems, *Energy*, **101** (2016), 506–518.
52. T. P. Xuan, P. Siarry, H. Oulhadj, Integrating fuzzy entropy clustering with an improved PSO for MRI brain image segmentation, *Appl. Soft Comput.*, **65** (2018), 230–242.
53. Z. W. Ye, M. W. Wang, W. Liu, S. Chen, Fuzzy entropy based optimal thresholding using bat algorithm, *Appl. Soft Comput.*, **31** (2015), 381–395.
54. D. E. Dutkay, C. K. Lai, Uniformity of measures with Fourier frames, *Adv. Math.*, **252** (2014), 684–707.
55. K.G. Lore, A. Akintayo, S. Sarkar, LLNet: A deep autoencoder approach to natural low-light image enhancement, *Pattern Recogn.*, **61** (2017), 650–662.
56. M. Koppel, K. Muller, T. Wiegand, Filling disocclusions in extrapolated virtual views using hybrid texture synthesis, *IEEE Trans. Broadcast.*, **62** (2016), 1–13.
57. H. M. Jia, Z. K. Xing, W. L. Song, Three dimensional pulse coupled neural network based on hybrid optimization algorithm for oil pollution image segmentation, *Remote Sens.*, **11** (2019), 1046.
58. A. Ewees, M. Elaziz, D. Oliva, Image segmentation via multilevel thresholding using hybrid optimization algorithms, *J. Electron. Imag.*, **27** (2018), 1–26.
59. H. M. Jia, C. Lang, D. Oliva, S. Song, Dynamic harris hawks optimization with mutation mechanism for satellite image segmentation, *Remote Sens.*, **11** (2019), 1421.
60. M. Friedman, The use of ranks to avoid the assumption of normality implicit in the analysis of variance, *J. Am. Stat. Assoc.*, **32** (1939), 675–701.
61. B. Rosner, R. J. Glynn, M. Lee, Incorporation of clustering effects for the Wilcoxon rank sum test: A large-sample approach, *Biometrics*, **59** (2003), 1089–1098.
62. Y. Chen, S. K. Park, Y. Ma, A. Rajeshkanna, A new automatic parameter setting method of a simplified PCNN for image segmentation, *IEEE Trans. Neural Netw. Learn. Syst.*, **22** (2011), 880–892.
63. E. Rajaby, S. M. Ahadi, H. Aghaeinia, Robust color image segmentation using fuzzy c-means with weighted hue and intensity, *Digit. Signal Prog.*, **51** (2016), 170–183.
64. Z. K. Xing, H. M. Jia, Multilevel color image segmentation based on GLCM and improved Salp swarm algorithm, *IEEE Access*, **7** (2019), 37672–37690.

AIMS Press

©2021 the Author(s), licensee AIMS Press. This is an open access article distributed under the terms of the Creative Commons Attribution License (http://creativecommons.org/licenses/by/4.0)